

point phenomena in  $^3\text{He}$ - $^4\text{He}$  mixtures, such as recently reported by Alpern, Benda, and Leiderer,<sup>10</sup> may help to elucidate this behavior. Because our own measurements from initially phase-separated mixtures are not yet complete, we reserve until a later time a discussion of a direct intercomparison of that data.

In conclusion, we have shown that there is no anomalous behavior in the dynamics of homogeneous binary phase separation near the tricritical point of  $^3\text{He}/^4\text{He}$  mixtures.

We have benefitted from conversations with L. J. Campbell, K. Kawasaki, W. E. Keller, J. S. Langer, and J. L. Lebowitz. This work was supported by the U. S. Department of Energy.

<sup>1</sup>For a recent review, see Walter I. Goldberg, in *Scattering Techniques Applied to Supramolecular and Nonequilibrium Systems*, edited by S. M. Chen, B. Chu, and R. Nossal (Plenum, New York, 1981), p. 383.

<sup>2</sup>Dipen N. Sinha and James K. Hoffer, *Physica* (Utrecht) **107B**, 155 (1981).

<sup>3</sup>Th. Benda, P. Alpern, and P. Leiderer, *Physica*

(Utrecht) **107B**, 157 (1981).

<sup>4</sup>Th. Benda, P. Alpern, and P. Leiderer, *Phys. Rev. B* **26**, 1450 (1982).

<sup>5</sup>J. del Cueto, R. L. Johnson, T. Rhode, F. H. Wirth, and E. H. Graff, *J. Phys. (Paris)*, Colloq. **41**, C7-133 (1980); P. Leiderer, private communications. The tricritical parameters,  $X_t(P)$  and  $T_t(P)$ , were determined from an interpolation of data from these two sources.

<sup>6</sup>P. Leiderer, D. R. Watts, and W. W. Webb, *Phys. Rev. Lett.* **33**, 43 (1974); P. Leiderer, D. R. Nelson, D. R. Watts, and W. W. Webb, *Phys. Rev. Lett.* **34**, 1080 (1975). Although our  $^3\text{He}$ - $^4\text{He}$  mixture is sometimes a homogeneous *normal* phase before the quench, the mixture must convert to the *superfluid* phase just prior to phase separation (see Fig. 2). Therefore, we assume that the values of  $D$  and  $\xi$  given in these references, which are for the superfluid phase only, are appropriate.

<sup>7</sup>E. Siggia, *Phys. Rev. A* **20**, 595 (1979).

<sup>8</sup>In Ref. 3, asymmetry in the halo pattern was observed in the late stages. However, the patterns we observe are uniformly circular as verified by cinematography taken at 50 frames per second.

<sup>9</sup>G. Ahlers and D. S. Greywall, *Low Temperature Physics, LT-13* (Plenum, New York, 1974), Vol. 1, p. 586.

<sup>10</sup>P. Alpern, Th. Benda, and P. Leiderer, *Phys. Rev. Lett.* **49**, 1267 (1982).

## Surface Phonon Dispersion of Ni(100) Measured by Inelastic Electron Scattering

S. Lehwald, J. M. Szeftel,<sup>(a)</sup> and H. Ibach

*Institut für Grenzflächenforschung und Vakuumphysik, Kernforschungsanlage Jülich, D-5170 Jülich, West Germany*

and

T. S. Rahman and D. L. Mills

*Department of Physics, University of California, Irvine, California 92717*

(Received 29 November 1982)

The thermal diffuse background between diffracted electron beams has been analyzed with high-energy resolution. The main contribution arises from a surface phonon single-scattering event. The surface phonon dispersion is measured along the  $\bar{\Gamma}$ - $\bar{X}$  direction, and compared with theoretical models.

PACS numbers: 68.30.+z, 79.20.Kz

Fifteen years ago Webb and co-workers<sup>1</sup> investigated the scattering of electrons with a kinetic energy of several hundred electronvolts from clean silver surfaces, and concluded that the background between the diffraction spots was predominantly caused by phonon scattering. A theoretical discussion of single-phonon inelastic processes was provided by Roundy and Mills.<sup>2</sup> Sharp features in the energy spectrum of elec-

trons due to the excitation of surface phonons were predicted with additional broadbands arising from bulk phonons. Despite substantial improvements in high-resolution electron-energy-loss spectroscopy, the predicted phonon losses were not observed hitherto since previous high-resolution spectrometers were restricted to impact energies too low for an effective phonon scattering cross section, except for the special

situation when dipole scattering could be exploited.<sup>3</sup> A recent series of calculations<sup>4</sup> show that as the electron energy is raised from a few electronvolts to a few hundred electronvolts, the inelastic cross section consists of a background value which rises monotonically with increasing energy, upon which the fraction structure is superimposed; the cross sections can be appreciable near the high end of this energy range.

In this Letter we report the first high-resolution ( $\sim 7$  meV) energy-loss spectra from a surface with high impact energies (180 and 320 eV). Spectra taken on a Ni(100) surface show that between diffracted beams the scattering is mostly inelastic phonon scattering, dominated by a single-surface-phonon loss. The good signal-to-noise ratio in the spectra allows an accurate measurement of the dispersion relation of the surface phonon. The results reported here thus show that with appropriate choice of primary energy, electron-energy-loss spectroscopy may be used to probe the vibrational properties of clean surfaces throughout the two-dimensional Brillouin zone. The data are compared with theoretical studies of phonon dispersion curves, and spectral density calculations. We find good agreement between the data and simple lattice-dynamical models.

Simple Debye-Waller-factor considerations show that the total probability for a 200-eV electron to be inelastically scattered by a phonon is of the order of 20%, for Ni at 300 K. However the inelastic events are distributed in momentum and energy, and only a small fraction of the target current arrives at the detector in an experiment which resolves energy and momentum. Our experiments were performed by using a double-pass electron spectrometer as described earlier,<sup>5</sup> with a lens system which was modified to bring the focal plane closer to the sample. Thereby the acceptance angle was enlarged. The remaining resolution in momentum was  $\Delta q_{\parallel} \approx 0.01 \text{ \AA}^{-1}$  for an impact energy of  $E_0 = 180$  eV and an energy resolution of  $\sim 7$  meV. Single-crystal Ni(100) surfaces were prepared by following conventional procedures. This involved cycles of annealing and sputter cleaning until carbon and sulfur were leached off the entire sample. During the measurements, the vacuum was maintained in the  $10^{-12}$  Torr range. Surface structure, orientation, and cleanliness were controlled with use of low-energy electron diffraction and Auger spectroscopy.

The scattering geometry is illustrated in the

inset of Fig. 1. Electrons were collected with a fixed polar angle of  $\sim 70^\circ$  along the  $[\bar{1}10]$  azimuth ( $\bar{\Gamma}-\bar{X}$  direction) while the impinging beam was rotated between polar angles yielding (01) and (00) diffracted beams. Phonon losses were found in the entire range between (01) and (00) positions. Higher count rates were obtained, however, when the phonon dispersion curve along  $\bar{\Gamma}-\bar{X}$  was measured taking the (01) position as the  $\bar{\Gamma}$  point. This is easy to understand since the phonon scattering cross section contains a factor  $[(\vec{k}^{(I)} - \vec{k}^{(S)}) \cdot \vec{u}]^2$ ,<sup>2</sup> with  $\vec{k}^{(I)}$  and  $\vec{k}^{(S)}$  the wave vector of the initial and scattered electrons, respectively, and  $\vec{u}$  the vibrational amplitude. This factor is about 3 times larger at the (01) position than at the (00) position, for the geometry described above.

Sample spectra with  $q_{\parallel} = |\vec{k}_{\parallel}^{(I)} - \vec{k}_{\parallel}^{(S)} - \vec{G}_{\parallel}^{(01)}| = 0.4 \text{ \AA}^{-1}$  and  $q_{\parallel} = 1.26 \text{ \AA}^{-1}$  ( $\bar{X}$  point of the two-dimensional Brillouin zone) are shown in Fig. 2. One sees sharp features corresponding to phonon loss and gain in both spectra. The inelastic signal is much larger for  $q_{\parallel} = 0.4 \text{ \AA}^{-1}$ . This is partly due to the difference in  $\vec{k}^{(I)} - \vec{k}^{(S)}$ . The largest effect, however, is from the statistical factor  $[n(\omega) + 1](1/\omega)$  and  $n(\omega)(1/\omega)$  for phonon loss and

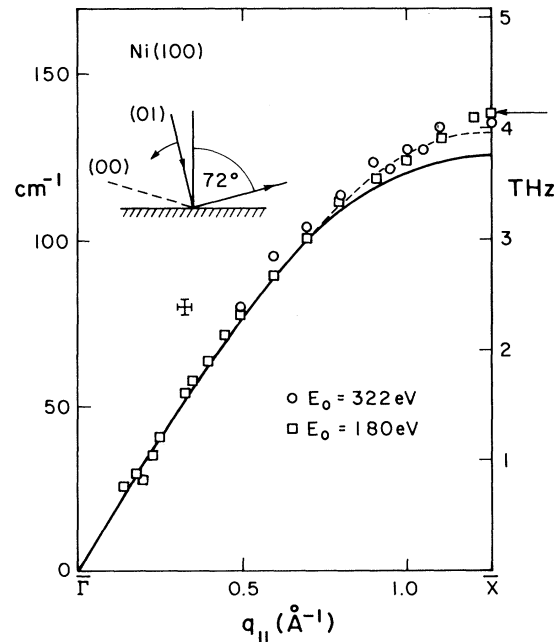


FIG. 1. Peak positions of the loss spectra vs  $q_{\parallel}$ . Data represent two sample runs for impact energies of 180 and 322 eV. The solid line is the dispersion curve calculated from the nearest-neighbor central-force model, with force constant chosen to fit the bulk phonon spectrum. The dashed line is with a 20% increase in the force constant between the first and second layers.

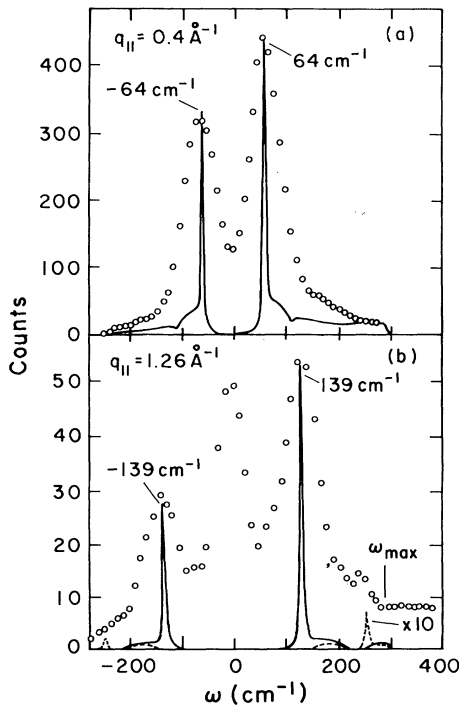


FIG. 2. Sample spectra for  $q_{||} = 0.4 \text{ \AA}^{-1}$  and  $1.26 \text{ \AA}^{-1}$  ( $\bar{X}$  point), as obtained with a beam energy of 180 eV. Data are digitally smoothed. The sampling time was 10 sec per point. Note that the elastic diffuse scattering is relatively small. The solid lines in (a) and (b) are the spectral densities for the vertical motion of atoms in the first layer. The dashed line in (b) represents the spectral density of the parallel motion weighted with the ratio of  $(\bar{k}_{||}(I) - \bar{k}_{||}(S))^2 / (k_{||}(I) - k_{||}(S))^2$ .

gain, respectively, with  $n(\omega) = [\exp(\hbar\omega/kT) - 1]^{-1}$ . Because of this factor, and because of the improvement in the resolving power of the experiment when both phonon loss and gain are strongly excited, all measurements were made with the crystal at room temperature rather than at low temperatures. Higher temperatures would have brought about further improvement in the signal, but with the danger of faster contamination of the sample. Typical recording times of the spectra were 15 min, with 10 sec sampling time for each channel. Thus an entire dispersion curve can be measured in a one-day shift. For an accurate determination of the surface phonon frequency, the data were digitally smoothed and the peak positions were determined by a least-squares fit with Gaussians. The precision of the procedure is about  $\pm 2 \text{ cm}^{-1}$  ( $6 \times 10^{10} \text{ sec}^{-1}$ ) and thus comparable to the precision of neutron scattering from bulk phonons.<sup>6</sup> The  $q_{||}$  scale was calibrated with the diffracted beams and is assumed to be

accurate to  $\pm 0.02 \text{ \AA}^{-1}$  in between

The peak positions as a function of  $q_{||}$  are plotted in Fig. 1, and we find that the data coincide closely with that of the  $S_4$  surface phonon discussed first by Allen, Aldredge and de Wette.<sup>7</sup> The solid curve in Fig. 1 is the dispersion relation of this mode, as given by the simple nearest-neighbor central-force model, with its single parameter adjusted to fit the maximum bulk Ni phonon frequency, and no changes in force constants for the surface. The fit is remarkably good, save for a small discrepancy near  $\bar{X}$ . If the force constant which couples atoms in the first layer to those in the second is increased 20% to mimic a modest inward relaxation of the surface layer, then the dashed curve is obtained. This fits the data throughout the two-dimensional Brillouin zone even more closely. Black, Campbell, and Wallis<sup>8</sup> have explored a more sophisticated model with angle-bending interactions included, and the frequency they calculate at  $\bar{X}$  for  $S_4$  (with no changes in surface force constants) is indicated by an arrow in Fig. 1. The result is in remarkable accord with the data, so that it is not clear if surface relaxation need be invoked. On the basis of the dispersion curve alone, we have no means of deciding which of the above two pictures most correctly describes the surface region. We favor the possibility of a small inward contraction of the surface layer on physical grounds, and so subsequent considerations here will be based on the nearest-neighbor model, with stiffened force constant (20%) between the first and second layer.

In addition to  $S_4$ , for which the atomic displacement at  $\bar{X}$  is normal to the surface in the outermost layer,<sup>9</sup> we have a shear polarized surface phonon  $S_1$  ( $\vec{u}$  parallel to surface and perpendicular to  $\vec{q}_{||}$ ). Selection rules applicable to the impact scattering regime<sup>4</sup> show that this mode is forbidden to scatter in the present geometry, and we find no evidence for it in the data. A third mode,  $S_6$ , exists near  $\bar{X}$  and is allowed (displacement in surface layer parallel to  $\vec{q}_{||}$  and to the surface), but the kinematical argument outlined above suggests the  $S_6$  excitation cross section is smaller than that for  $S_4$  by a factor of 25, at  $\bar{X}$ . We comment further on this below.

We have carried out a series of spectral density calculations, similar to those reported earlier for the (111) surface,<sup>10</sup> to explore the influence of  $S_4$  on the frequency spectrum of the surface layer vibrations, along the line from  $\bar{\Gamma}$  to  $\bar{X}$ . Since  $S_4$  lies very close to the appropriate

bulk phonon continuum<sup>11</sup> throughout a substantial portion of this region of the zone, it is not clear *a priori* if it provides the dominant feature in the spectral density; bulk vibrations may possibly contribute prominently in this circumstance.<sup>2</sup> The solid lines in Fig. 2(a) are calculations of the frequency spectrum of fluctuations in the displacements normal to the surface for wave vector  $q_{\parallel} = 0.4 \text{ \AA}^{-1}$ , for atoms in the outermost substrate layer. We have used the nearest-neighbor central-force model, with the force constant between first and second layer stiffened by 20%, for the reason discussed above. The prominent peaks are produced by the  $S_4$  mode; the structure is broadened by introducing an imaginary part of  $6 \text{ cm}^{-1}$  to the frequency, and as this damping rate is decreased, the peaks produced by  $S_4$  narrow accordingly. One also sees a wing on the high-frequency side of the  $S_4$  mode with origin in the bulk phonon continuum. This is reproduced in the data. In Fig. 2(b), the features at  $\pm 139 \text{ cm}^{-1}$  are again produced by the  $S_4$  mode (at  $\bar{X}$ ), which has only a normal component of displacement at that point. We also show a calculation of the frequency spectrum, at  $\bar{X}$ , associated with displacements parallel to the surface, and to  $\vec{q}_{\parallel}$ . The peak in the theoretical spectrum at  $252 \text{ cm}^{-1}$  is associated with the  $S_6$  mode, and a feature appears in the data near this frequency. It is not clear if the feature in the data is truly  $S_6$ ; an estimate of its intensity with kinematical theory suggests that the line should be weaker by one order of magnitude, and the mode would be unobservable if this estimate were correct. Also, the count rate in this region of the loss spectrum is too low for the precise position and line shape of this feature to be determined in an unambiguous fashion.

Measurements of surface phonon dispersion for LiF and Au with inelastic scattering of helium atoms<sup>12,13</sup> have been reported earlier. Although the energy resolution obtained with this technique is higher than in electron scattering, the atomic beam method can so far be used only for non-reactive surfaces, and the frequencies of the

phonons so studied are restricted by the low energy of the beam. In electron spectroscopy, there are no such constraints. It is thus possible to study the dispersion of high-frequency adsorbate vibrations. Such data on ordered oxygen overlayers on Ni(100) have been obtained, and will be reported in a subsequent publication.

One of us (J.M.S.) wishes to thank the Alexander von Humboldt Foundation for fellowship support. This work has also been supported by the U. S. Department of Energy, through Contract No. DEAT 0379-ER-10432.

(a)Permanent address: S. P. A. S., Centre d'Etudes Nucléaires de Saclay, F-91191 Gif-sur-Yvette Cédex, France.

<sup>1</sup>J. T. Mc Kinney, E. R. Jones, and M. B. Webb, Phys. Rev. **160**, 523 (1967).

<sup>2</sup>V. Roundy and D. L. Mills, Phys. Rev. B **5**, 1347 (1972).

<sup>3</sup>H. Ibach, Phys. Rev. Lett. **24**, 1416 (1970), and **27**, 253 (1971).

<sup>4</sup>S. Y. Tong, C. H. Li, and D. L. Mills, Phys. Rev. Lett. **44**, 407 (1980), and Phys. Rev. B **24**, 806 (1981).

<sup>5</sup>See Chap. 2 of *Electron Energy Loss and Surface Vibrations*, edited by H. Ibach and D. L. Mills (Academic, San Francisco, 1982).

<sup>6</sup>R. J. Birgenau, J. Cordes, G. Dolling, and A. D. B. Woods, Phys. Rev. A **136**, 1359 (1964).

<sup>7</sup>R. E. Allen, G. P. Alldredge, and F. W. de Wette, Phys. Rev. B **4**, 1661 (1971).

<sup>8</sup>J. E. Black, D. A. Campbell, and R. F. Wallis, Surf. Sci. **115**, 161 (1982).

<sup>9</sup>In Chap. 5 of Ref. 3 a detailed discussion is given of surface phonons at  $\bar{X}$ , on the (100) surface of an fcc crystal.

<sup>10</sup>J. E. Black, T. S. Rahman, and D. L. Mills, Phys. Rev. B, to be published.

<sup>11</sup>Near  $\bar{\Gamma}$ ,  $S_4$  lies *within* the continuum of bulk shear polarized phonons with displacement parallel to the surface and normal to the  $\bar{\Gamma}$ - $\bar{X}$  line. However, it is decoupled from these modes by symmetry. As one moves to  $\bar{\Gamma}$  and  $\bar{X}$ ,  $S_4$  comes very close to the continuum of bulk phonons with displacement parallel to the sagittal plane.

<sup>12</sup>G. Brusdeylins, R. Bruce Doak, and J. Peter Toennis, Phys. Rev. Lett. **46**, 437 (1981).

<sup>13</sup>M. Cates and D. R. Miller, to be published.